Journal of Materials Chemistry C

ROYAL SOCIETY OF CHEMISTRY

PAPER

View Article Online
View Journal | View Issue

Cite this: J. Mater. Chem. C, 2025, 13, 19417

Adjustment and detection of the topology freezing transition temperature of vitrimers based on vitrimers doped with nanoparticles and photonic crystals

Jie Miao,†[a] Wenxiao Long,†[a] Jiayi Yan[a] and Chengjia Xiong *[ab]

Received 9th May 2025,
Accepted 11th August 2025

DOI: 10.1039/d5tc01866h

rsc.li/materials-c

The topology freezing transition temperature (T_v) of vitrimers is an important indicator for their applications. The T_v of vitrimers could be changed by using chemical methods. Herein, a physical method is proposed to adjust and detect the T_v of vitrimers based on upper vitrimers doped with SiO_2 nanoparticles and lower photonic crystals (PCs) from SiO_2 nanoparticles. When the photonic coatings are heated, the upper vitrimers changed from a viscoelastic-solid state to a viscoelastic-liquid state, and the reflection peak intensities of the PCs increased because light easily penetrated the coatings. The T_v of vitrimers could be determined according to changes in the peak intensities. When the photonic coatings are synthesized at 140 °C for 6 h under 2.6 MPa, the lower PCs exhibited no change, and as the doping amounts of SiO_2 nanoparticles in the upper vitrimers are increased, the T_v of the photonic coatings decreased from 90 °C to 72.5 °C. The photonic coatings have potential applications in adjustment and detection of T_v of other vitrimers, anti-counterfeiting and displays.

Introduction

Vitrimers were first reported by Leibler *et al.*[1] Vitrimers are covalently crosslinked, and they have many advantages. For example, vitrimers could be recycled upon heating at temperatures higher than their topology freezing transition temperature (T_v). When the heating temperature is lower than the T_v, vitrimers are similar to thermoset materials, and they will woke fine. Because the T_v of vitrimers is an important indicator for their applications, its detection is extremely important. There are a few methods to determine the T_v of vitrimers. For example, Ji *et al.* developed a method to detect T_v by doping aggregation-induced-emission (AIE) luminogens into vitrimers.[2] A rheology[1] or dynamic mechanical analyzer[3] is used for detecting the T_v of vitrimers based on a dilatometry or stress-relaxation test, respectively, but the vitrimers are under the influence of external forces in these two methods, which may affect the values of T_v.[2] Because photonic crystals (PCs) are materials with photonic band gaps, they have been used in many areas, such as environment-friendly photonic coatings (or pigments),[4,5] color displays,[6–12] inkless rewritable papers,[13,14] cellular (or adhesive) force monitoring,[15,16] and chemical (or biological) detection.[17–25] The photonic coatings from lower PCs and upper vitrimers were used to detect the T_v of vitrimers in our previous study.[26] The above-mentioned method is simple, without using external forces and additional substances, but the T_v of vitrimers could not be changed by this method.

The T_v of vitrimers could be changed by chemical methods.[27,28] For example, Ji *et al.* synthesized different chemicals (epoxy vitrimers, polyurethanes and polyimine) to adjust the T_v of vitrimers.[2] Poly(ethylene-α-octene) (POE) vitrimers were synthesized, and their T_v values were changed by introducing the dynamic dioxaborolane cross-links into the commercial pure POE.[27] Different kinds of chemicals result in different T_v values. Herein, a physical approach is proposed to adjust and detect the T_v of vitrimers based on upper vitrimers doped with SiO_2 nanoparticles and lower PCs from SiO_2 nanoparticles. Meanwhile, the detection of the T_v of vitrimers is achieved according to the intensity changes in the reflection peaks of the photonic coatings when they are heated.

Experimental section

Materials

Ethanol, ammonia, triazobicyclodecene, diglycidyl ether of bisphenol, dodecanedioic acid and tetraethoxysilane (TEOS) are purchased from Shanghai Aladdin Corporation. All chemicals are of analytical grade and used without further purification.

[a] School of Building and Materials Engineering, Hubei University of Education, Wuhan 430205, P. R. China. E-mail: cjxiong@iccas.ac.cn
[b] Hubei Engineering Technology Research Center of Environmental Purification Materials, Hubei University of Education, 430205 Wuhan, P. R. China
† These authors contributed equally to this work.

Synthesis of SiO_2 spheres and fabrication of PCs

Monodispersed SiO_2 spheres are synthesized by the Stöber method.[29] Typically, 42 mL of ethanol, 16 mL of deionized water and 8 mL of aqueous ammonia are mixed and stirred for 30 min; then, 1.8 mL of TEOS is dripped into this mixture solution. The solution is stirred at 25 °C for 16 h, and monodispersed SiO_2 spheres are obtained. The PCs are fabricated using an optimized vertical deposition method based on multiple glass slides of a simple mould, as reported in our previous study.[30] Typically, 0.04 g of SiO_2 spheres is ultrasonically dispersed in 15 mL of ethanol. A simple mould inserted with multiple glass substrates is immersed in the SiO_2 dispersion solution, and then, it is evaporated at a stable temperature of 64 °C for 18 h. Finally, uniform PC films on glass slide substrates are obtained.

Fabrication of PCVD coatings

Epoxy vitrimers are prepared according to previous reports,[2,31] and photonic coatings are fabricated following the method in our previous work.[26] The detailed fabrication procedure of PCVD coatings (PCs and vitrimers doped with SiO_2 nanoparticles) is as follows: typically, triazobicyclodecene (0.01 g, 0.07 mmol) is put on the margin of a glass sheet with PCs. Next, 5×10^{-4} g of SiO_2 nanoparticles (moderate amounts) is ultrasonically dispersed in 2 mL of ethanol; SiO_2 dispersion, diglycidyl ether of bisphenol A (0.25 g, 0.73 mmol) and dodecanedioic acid (0.18 g, 0.78 mmol) are ultrasonically dispersed and heated at 155 °C for 30 min. 15 drops of the mixture are added onto the surface of triazobicyclodecene. The side with the mixture of glass sheets is inclined upward at an angle of 4° and heated at 155 °C for 20 min, which made the mixture overspread on the PCs. After that, the margin of the glass sheet is put downwards, the other end of the glass sheet is inclined upward at an angle of 11°, and the coating is heated at 155 °C for 20 min. An appropriate thickness of photonic coatings is achieved by this method. Then, the film is heated at 140 °C for 8 h. Finally, the film is put in a high-pressure kettle that is filled with N_2; the PCVD coating is obtained when the heating temperature is 140 °C for 6 h and the pressure of the kettle is 2.6 MPa.

Detection of the T_v of PCVD coatings

The schematic and real-time detection of the T_v of the PCVD coatings were illustrated in our previous report.[26] Typically, a PCVD film is put on a big glass sheet (support function). The temperature of the big glass sheet is controlled by an oil-bath pan. The big glass sheet and PCVD film are heated, and the temperatures are kept constant for 10 min to ensure full heat exchange. Then, *in situ* reflection spectra of the PCVD coatings are obtained by an optical spectrometer at normal incidence.

Material characterizations

Reflection spectra of the PCs and photonic coatings are obtained using an optical spectrometer (QEPRO, Ocean Optics,

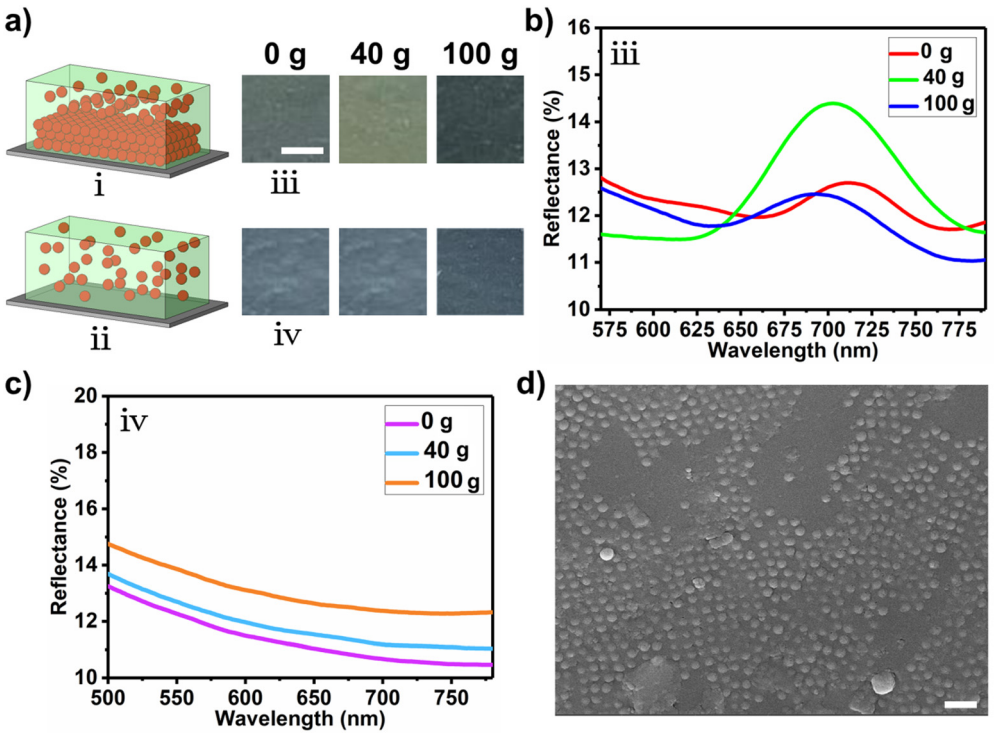

Fig. 1 (a) Schematic of the two kinds of photonic coatings: (i) photonic coating made from the upper vitrimers doped with nanoparticles and lower PCs from nanoparticles and (ii) photonic coating made from vitrimers and amorphous PCs. (iii) and (iv) Photographs of the two kinds of coatings doped with SiO_2-1 nanoparticles after being loaded with different weights under 140 °C for 1 h. Scale bar: 1 mm. (b) and (c) Reflection spectra of the two kinds of photonic coatings under different pressures. (d) Cross-sectional SEM image of the first kind of photonic coating from vitrimers and SiO_2-2 nanoparticles. Scale bar: 1 μm.

USA). Photographs are taken with a smartphone (iPhone 12, USA). Scanning electron microscopy images are obtained using TESCAN MIRA LMS (Czech Republic).

Results and discussion

Two kinds of photonic coatings are fabricated. The first photonic coating is made from the upper vitrimers doped with SiO_2 nanoparticles and lower PCs from SiO_2 nanoparticles (Fig. 1a, i); the second photonic coating consists of vitrimers and amorphous SiO_2 PCs (Fig. 1a, ii), and it has no lower PCs. For the first kind of photonic coating obtained from vitrimers and SiO_2-1 nanoparticles, when the photonic coating is pressed by a 40 g weight and heated at 140 °C for 1 h, its structural color changed noticeably, and the structural color continues to change after-weight is up to 100 g (Fig. 1a, iii). For the second photonic coating synthesized from vitrimers and amorphous PCs, although the photonic coatings have structural colors in their original state, the changes in the structural colors are not obvious after they are pressed (Fig. 1a, iv). The reflection position of the first kind of photonic coating (iii) shifted from 711 nm to 702 nm and 691 nm after it is pressed (Fig. 1b). According to Bragg's law, $\lambda = 2d\sqrt{{n_{\text{eff}}}^2 - \sin^2\theta}$, where λ is the diffraction wavelength, n_{eff} is the effective refractive index, d is the interparticle distance, and θ is the angle of measurement with respect to the vector normal to the close-packed planes,[30] the blue shifts (λ) are due to the decrease in the lattice spacing (d) of the nanoparticles in the vertical direction.[13,32] Because the second kind of photonic coating (iv) has no lower PCs, there are no reflection peaks, and the changes in the reflection peaks are not obvious after it is pressed (Fig. 1c). Thus, the first kind of photonic coating is mainly investigated in this work. It is named as PCVD coating. Fig. 1d shows the representative cross-sectional SEM image of the first kind of photonic coating obtained from the vitrimers and SiO_2-2 nanoparticles. From the SEM image, the nanoparticles are monodispersed, and their average diameter is about 320 nm. These SiO_2 nanoparticles are completely embedded into the vitrimers, and the order of the degree of arrangement of SiO_2 nanoparticles in the vitrimers is high. A small part of the vitrimers is not filled by the nanoparticles as the doping amount of nanoparticles is very little.

The T_v and glass transition temperature (T_g) are two important parameters of vitrimers. The T_g of vitrimers without PCs was tested in a previous study, and it was about 45 °C.[2] The T_v of vitrimers is determined according to the changes in the reflection peaks of PCVD coatings when they are heated. PCVD coatings are synthesized at 140 °C for 6 h under 2.6 MPa; their reflection spectra and the corresponding intensity plots of the photonic coatings at different temperatures are shown in Fig. 2. The lower PCs are fabricated with the same amount of SiO_2 nanoparticles in the same beaker, and the upper vitrimers are doped with different amounts of SiO_2 nanoparticles (Fig. 2a). When excessive SiO_2 nanoparticles (1×10^{-3} g) are doped into the upper vitrimers, the color of the PCVD coatings inclined to white, which is derived from the color of the SiO_2 nanoparticles (Fig. S1). When moderate amounts of SiO_2 nanoparticles (5×10^{-4} g) are doped into the upper vitrimers, the structural colors of the PCVD coatings are almost unchanged compared with those of the photonic coatings without nanoparticles. When the doping amount of SiO_2 nanoparticles is 2.5×10^{-4} g, it is considered as a small amount of SiO_2 nanoparticles. When PCVD coatings are heated and the heating temperature is higher than the T_v of vitrimers, the chemical property of the SiO_2 spheres remains stable, the vitrimers gradually transform from a viscoelastic-solid state to a viscoelastic-liquid state, and light easily penetrates the vitrimers and reflects off the PCs under the viscoelastic-liquid state.[25] Therefore, the intensities of the reflection peaks of all the PCVD coatings would increase sharply when the states of the vitrimers are changed. The beginning temperature is the temperature at which the intensity of the reflection peaks of the PCVD coatings begins to increase, while the finishing temperature is that at which the intensity of the reflection peaks remains almost unchanged. The T_v is the average temperature between the beginning and finishing temperatures. The representative T_v is marked in Fig. 2b. PCs-1 and PCs-2 are obtained from SiO_2-1 and SiO_2-2 nanoparticles, and the reflection peaks of the two PCs are located at 633 nm and 731 nm, respectively (Fig. S2). The reflection peak intensities of the two PCs are higher than 50%, and according to our previous work, this indicates that the SiO_2 spheres are monodispersed.[30] This conclusion is in agreement with the result shown in Fig. 1d. After vitrimers are added to the surfaces of PCs-1 and PCs-2, the positions of the reflection peaks of the PCVD coatings are 698 nm and 809 nm, respectively. When the lower PCs-1 are the same and the upper vitrimers are doped by small, moderate and excessive amounts of SiO_2-1 nanoparticles, respectively, the values of the T_v of PCVD coatings are 90 °C (Fig. 2b), 85 °C (Fig. 2c) and 72.5 °C (Fig. 2d), respectively. The T_v values of the PCVD coatings decrease as the doping amounts of SiO_2 nanoparticles increase. In order to prove the reliability of the results, other batches of PCVD coatings are synthesized at 140 °C for 6 h under 2.6 MPa (named as PCVD-1-2, PCVD-1-3, *etc.*), and their T_v values are investigated. For result analysis, serial numbers of PCVD coatings and their T_v values are summarized in Table S1. The T_v values of PCVD-1-2, PCVD-2-2 and PCVD-3-2 are 90 °C (Fig. S3a), 80 °C (Fig. S3b) and 75 °C (Fig. S3c), respectively. The T_v values of PCVD-1-3, PCVD-2-3 and PCVD-3-3 are 90 °C (Fig. S4a), 85 °C (Fig. S4b) and 80 °C (Fig. S4c), respectively. It is found that the T_v values of different batches of PCVD coatings also decrease as the doping amounts of SiO_2 nanoparticles increase. Additionally, the T_v values of different batches of PCVD coatings synthesized under same conditions are very close, which indicates that the method is reliable. When PCVD coatings are obtained from the other SiO_2 nanoparticles, the lower PCs-2 from SiO_2-2 are the same and the upper vitrimers are doped by small, moderate and excessive amounts of SiO_2-2 nanoparticles, their values of T_v are 80 °C (Fig. 2e), 75 °C (Fig. 2f) and 65 °C (Fig. 2g), respectively. For different batches of the PCVD coatings from the SiO_2-2 nanoparticles, the T_v of PCVD-4-2, PCVD-5-2 and PCVD-6-2 are 75 °C (Fig. S3d), 62.5 °C (Fig. S3e) and

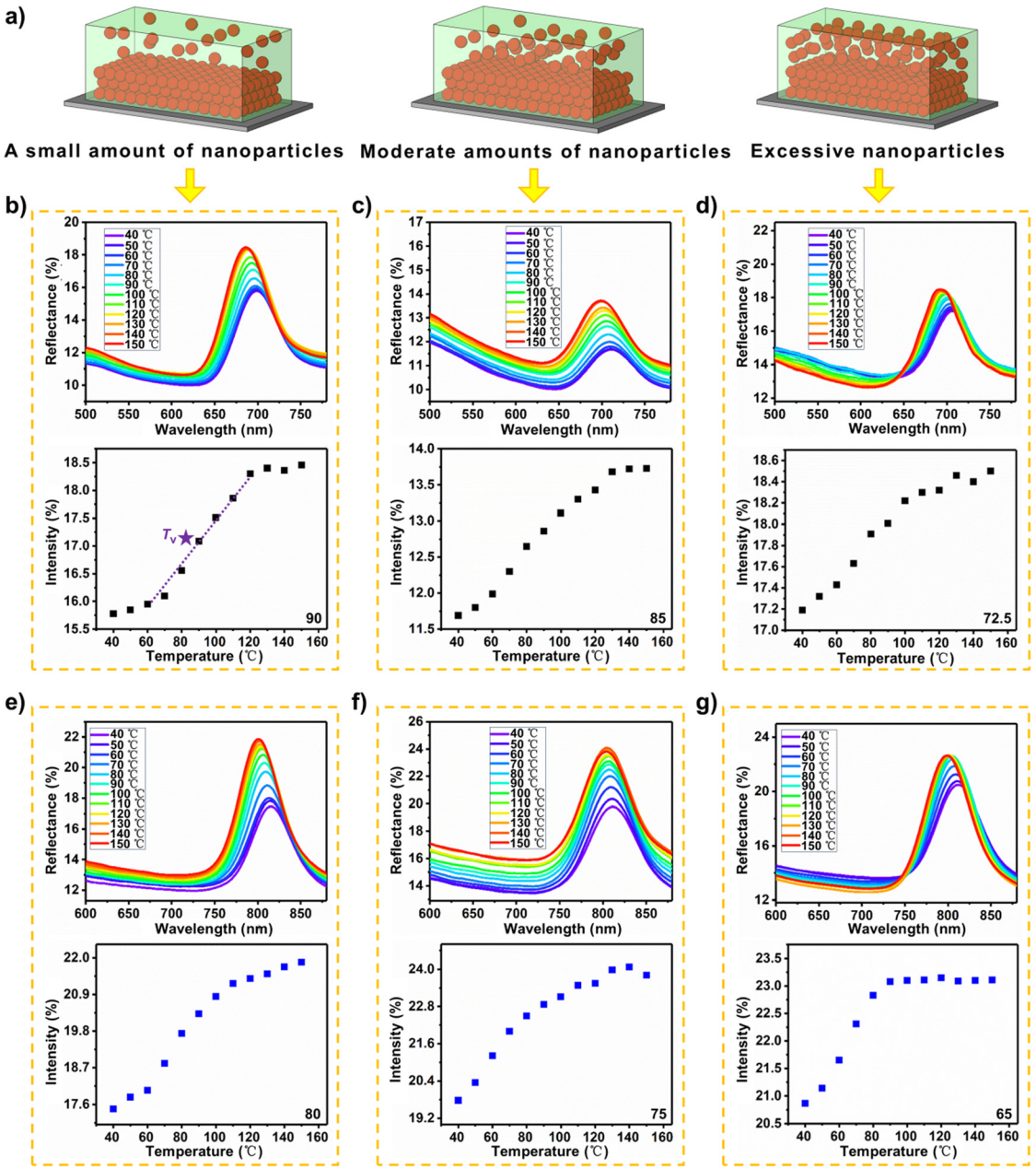

Fig. 2 Reflection spectra and the corresponding intensity plots of the PCVD coatings at different temperatures when the PCVD coatings are synthesized at 140 °C for 6 h under 2.6 MPa. (a) Schematic of the upper vitrimers doped with different amounts of SiO_2 nanoparticles and lower PCs from SiO_2 nanoparticles. Reflection spectra and the corresponding intensity plots of the PCVD coatings at different temperatures: the lower PCs are from SiO_2-1 nanoparticles, and the SiO_2-1 doping amounts of the upper vitrimers are (b) small, (c) moderate, and (d) excessive. Reflection spectra and the corresponding intensity plots of the PCVD coatings at different temperatures: the lower PCs are from SiO_2-2 nanoparticles, the SiO_2-2 doping amounts of the upper vitrimers are (e) small, (f) moderate, and (g) excessive.

60 °C (Fig. S3f), respectively. The T_v values of PCVD-4-3, PCVD-5-3 and PCVD-6-3 are 70 °C (Fig. S4d), 62.5 °C (Fig. S4e) and 62.5 °C (Fig. S4f), respectively. For the PCVD coatings from vitrimers and nanoparticles of different diameters, the T_v values decrease as the doping amounts of the nanoparticles increase. However, the extent of decrease in the T_v values of PCVD coatings from nanoparticles of different sizes is different. Reduction extent of the T_v is more obvious for PCVD coatings from smaller nanoparticles, while under the same conditions, T_v is smaller for PCVD coatings from SiO_2 nanoparticles with larger diameters. Therefore, the T_v of vitrimers is related to the doping amounts and diameters of the SiO_2 nanoparticles.

When the PCVD coatings are synthesized at 180 °C for 4 h under 3.0 MPa, their reflection spectra and the corresponding intensity plots at different temperatures are shown in Fig. 3. The lower PCs are fabricated with the same amounts of SiO_2 nanoparticles in the same beaker, and the upper vitrimers are

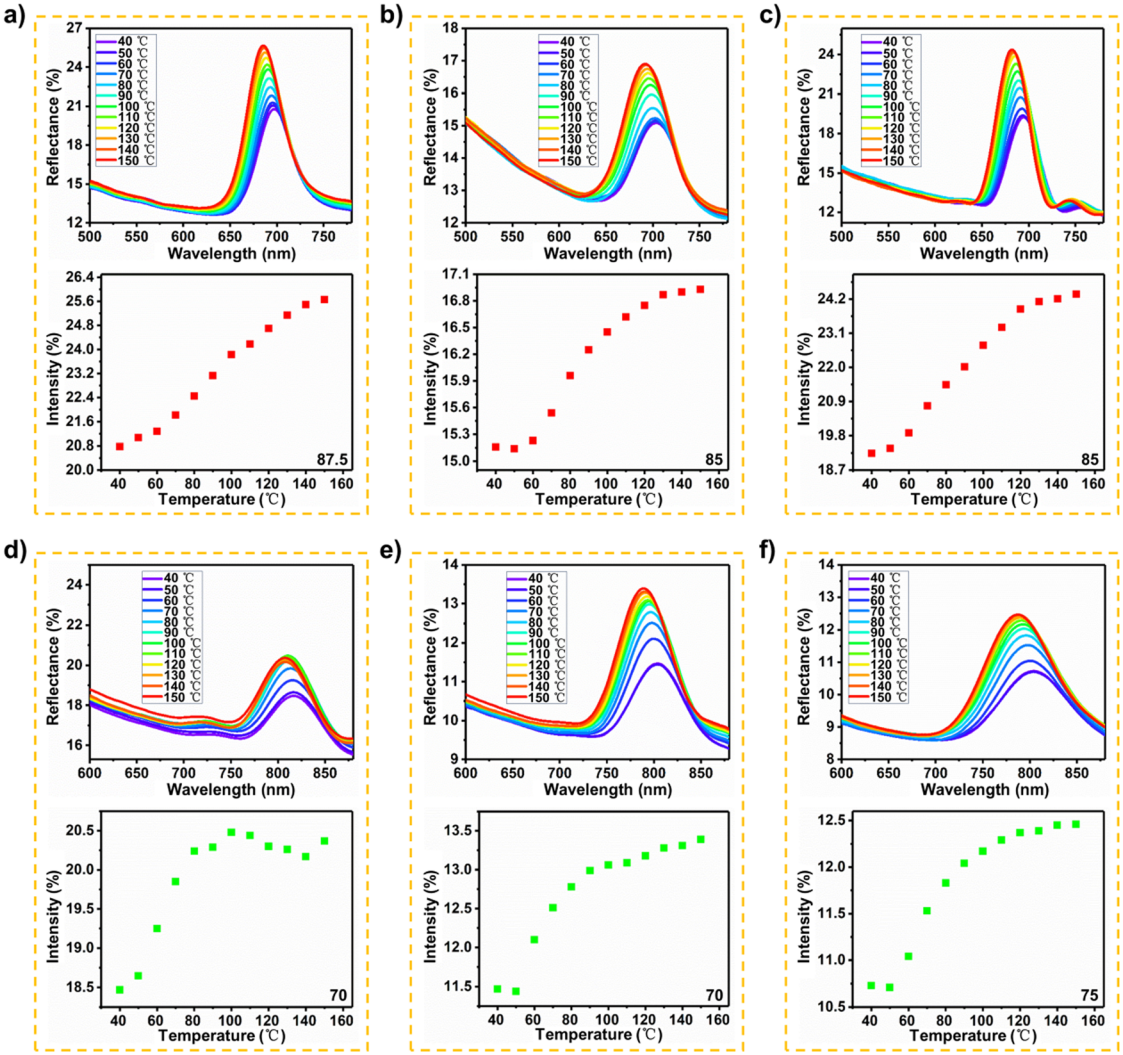

Fig. 3 Reflection spectra and the corresponding intensity plots of the PCVD coatings at different temperatures when the PCVD coatings are synthesized at 180 °C for 4 h under 3.0 MPa. Reflection spectra and the corresponding intensity plots of the PCVD coatings at different temperatures; the lower PCs are from SiO_2-1 nanoparticles, and the SiO_2-1 doping amounts of the upper vitrimers are (a) small, (b) moderate, and (c) excessive. Reflection spectra and the corresponding intensity plots of the PCVD coatings at different temperatures; the lower PCs are from SiO_2-2 nanoparticles, and the SiO_2-2 doping amounts of the upper vitrimers are (d) small, (e) moderate, and (f) excessive.

doped with different amounts of SiO_2 nanoparticles. When small, moderate, and excessive amounts of SiO_2-1 nanoparticles are doped into the upper vitrimers, the T_v values of PCVD-7-1, PCVD-8-1 and PCVD-9-1 are 87.5 °C (Fig. 3a), 85 °C (Fig. 3b) and 85 °C (Fig. 3c), respectively. Other batches of PCVD coatings are synthesized at 180 °C for 4 h under 3.0 MPa, and their T_v values are investigated. The T_v values of PCVD-7-2, PCVD-8-2 and PCVD-9-2 are 85 °C (Fig. S5a), 87.5 °C (Fig. S5b) and 87.5 °C (Fig. S5c), respectively. The T_v values of PCVD-7-3, PCVD-8-3 and PCVD-9-3 are 85 °C (Fig. S6a), 85 °C (Fig. S6b) and 80 °C (Fig. S6c), respectively. For the PCVD coatings from the SiO_2-2 nanoparticles and vitrimers, the T_v values of PCVD-10-1, PCVD-11-1 and PCVD-12-1 are 70 °C (Fig. 3d), 70 °C (Fig. 3e) and 75 °C (Fig. 3f), respectively. Other batches of PCVD coatings from the SiO_2-2 nanoparticles and vitrimers are synthesized at 180 °C for 4 h under 3.0 MPa. The T_v values of PCVD-10-2, PCVD-11-2 and PCVD-12-2 are 82.5 °C (Fig. S5d), 67.5 °C (Fig. S5e) and 70 °C (Fig. S5f), respectively. The T_v values of PCVD-10-3, PCVD-11-3 and PCVD-12-3 are 72.5 °C (Fig. S6d), 65 °C (Fig. S6e) and 62.5 °C (Fig. S6f), respectively. The T_v values of the PCVD coatings from SiO_2 nanoparticles with larger diameters are smaller than those from small-diameter nanoparticles under the same conditions, and the experimental phenomenon is the same as that in Fig. 2. But the changes in T_v are very small as the doping amounts of SiO_2 are increased, which is different from that of Fig. 2. The possible reason is that the curing degree of vitrimers is higher under higher pressure and temperature. Therefore, the T_v values of vitrimers are not easy to be adjusted by doping with SiO_2 nanoparticles. The above-mentioned results indicate that the adjustment of T_v is also related with to the synthesis condition of the vitrimers.

The second and third thermal responsive experiments of the same PCVD coatings are investigated. When moderate amounts of SiO_2 nanoparticles are doped into the upper vitrimers, the

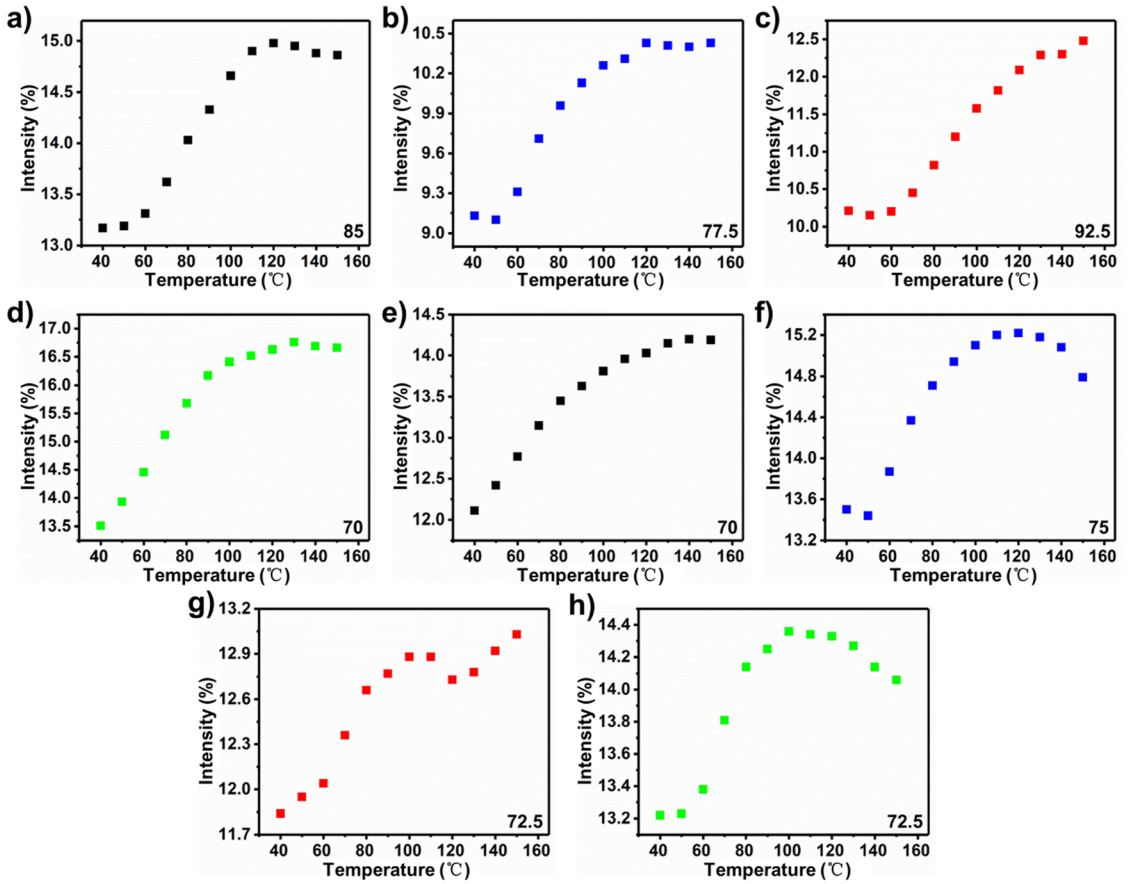

Fig. 4 Second and third thermal responsive results for different PCVD coatings when moderate amounts of nanoparticles are doped into the upper vitrimers. The second thermal responsive results: intensity plots of the reflection peaks of the (a) PCVD-2-1, (b) PCVD-5-1, (c) PCVD-8-2 and (d) PCVD-11-2 coatings at different temperatures. The third thermal responsive results: intensity plots of the reflection peaks of the (e) PCVD-2-1, (f) PCVD-5-1, (g) PCVD-8-2 and (h) PCVD-11-2 coatings at different temperatures.

second determined T_v values of the PCVD-2-1, PCVD-5-1, PCVD-8-2 and PCVD-11-2 coatings are 85 °C (Fig. 4a and Fig. S7a), 77.5 °C (Fig. 4b and Fig. S7b), 92.5 °C (Fig. 4c and Fig. S7c) and 70 °C (Fig. 4d and Fig. S7d), respectively. The third determined T_v values of the PCVD-2-1, PCVD-5-1, PCVD-8-2 and PCVD-11-2 coatings are 70 °C (Fig. 4e and Fig. S7e), 75 °C (Fig. 4f and Fig. S7f), 72.5 °C (Fig. 4g and Fig. S7g) and 72.5 °C (Fig. 4h and Fig. S7h), respectively. When a small amount of SiO_2 nanoparticles is doped into the upper vitrimers, the second determined T_v values of the PCVD-1-1, PCVD-4-1, PCVD-7-3 and PCVD-10-3 coatings are 70 °C (Fig. S8a and Fig. S9a), 77.5 °C (Fig. S8b and Fig. S9b), 85 °C (Fig. S8c and Fig. S9c) and 75 °C (Fig. S8d and Fig. S9d), respectively. The third determined T_v values of the PCVD-1-1, PCVD-4-1, PCVD-7-3 and PCVD-10-3 coatings are 85 °C (Fig. S8e and Fig. S9e), 75 °C (Fig. S8f and Fig. S9f), 70 °C (Fig. S8g and Fig. S9g) and 70 °C (Fig. S8h and Fig. S9h), respectively. When excessive nanoparticles are doped into the upper vitrimers, the second determined T_v values of the PCVD-3-3, PCVD-6-3, PCVD-9-1 and PCVD-12-1 coatings are 65 °C (Fig. S10a and Fig. S11a), 85 °C (Fig. S10b and Fig. S11b), 85 °C (Fig. S10c and Fig. S11c) and 70 °C (Fig. S10d and Fig. S11d), respectively. The third determined T_v values of the PCVD-3-3, PCVD-6-3, PCVD-9-1 and PCVD-12-1 coatings are 80 °C (Fig. S10e and Fig. S11e), 72.5 °C (Fig. S10f and Fig. S11f), 72.5 °C (Fig. S10g and Fig. S11g) and 67.5 °C (Fig. S10h and Fig. S11h), respectively. The second and third determined T_v values of the same PCVD coatings are high and low, respectively, indicating that the vitrimers are different from thermoplastic materials and are not completely reversible materials. Thus, the T_v values of vitrimers synthesized under different conditions could be adjusted and detected by this simple physical method based on PCVD coatings.

Conclusions

In summary, photonic coatings are fabricated in this work from upper vitrimers doped with SiO_2 nanoparticles and lower PCs. A physical method is proposed to adjust and detect the topology freezing transition temperature of vitrimers based on the PCVD coatings. The T_v values of the vitrimers are related to doping amounts of the SiO_2 nanoparticles, diameter of the SiO_2 nanoparticles and synthesis conditions. For adjustments in the T_v of vitrimers, this physical method is more convenient and simpler than chemical methods. Furthermore, the photonic coatings have structural colors. Consequently, they can be used for the adjustment of the T_v of other vitrimers, with

potential applications in displays, anti-counterfeiting and automotive coatings in the future.

Author contributions

Jie Miao: investigation. Wenxiao Long: investigation. Jiayi Yan: supervision. Chengjia Xiong: investigation, validation, supervision, resources, project administration, methodology, conceptualization, funding acquisition, writing – original draft, writing – review & editing.

Conflicts of interest

The authors declare no conflict of interest.

Data availability

Supplementary material is available. See DOI: **https://doi.org/10.1039/d5tc01866h**

Acknowledgements

C. J. Xiong thanks the Scientific Research Foundation of Hubei University of Education for Talent Introduction (No. ESRC20220051) and Scientific and Technology Research Project of Hubei Provincial Education Department (Q20233004).

References

1 D. Montarnal, M. Capelot, F. Tournilhac and L. Leibler, Silica-Like Malleable Materials from Permanent Organic Networks, *Science*, 2011, **334**, 965–968.
2 Y. Yang, S. Zhang, X. Zhang, L. Gao, Y. Wei and Y. Ji, Detecting topology freezing transition temperature of vitrimers by AIE luminogens, *Nat. Commun.*, 2019, **10**, 3165.
3 Y. Yang, E. M. Terentjev, Y. Wei and Y. Ji, Solvent-assisted programming of flat polymer sheets into reconfigurable and self-healing 3D structures, *Nat. Commun.*, 2018, **9**, 1906.
4 S. Ma, Y. Wang, H. Zheng, L. Qi and C. Xiong, Environment-friendly coating with good weather resistance prepared by amorphous photonic crystals and water-dispersible resin, *Opt. Mater.*, 2023, **140**, 113908.
5 Z. Li, X. Wang, L. Han, C. Zhu, H. Xin and Y. Yin, Multicolor Photonic Pigments for Rotation-Asymmetric Mechanochromic Devices, *Adv. Mater.*, 2022, **34**, 2107398.
6 S. Jeon, Y. L. Kamble, H. Kang, J. Shi, M. A. Wade, B. B. Patel, T. Pan, S. A. Rogers, C. E. Sing, D. Guironnet and Y. Diao, Direct-ink-write cross-linkable bottlebrush block copolymers for on-the-fly control of structural color, *Proc. Natl. Acad. Sci. U. S. A.*, 2024, **121**, e2313617121.
7 K. Liu, H. Ding, S. Li, Y. Niu, Y. Zeng, J. Zhang, X. Du and Z. Gu, 3D printing colloidal crystal microstructures via sacrificial-scaffold-mediated two-photon lithography, *Nat. Commun.*, 2022, **13**, 4563.
8 J. B. Kim, C. Chae, S. H. Han, S. Y. Lee and S. H. Kim, Direct writing of customized structural-color graphics with colloidal photonic inks, *Sci. Adv.*, 2021, **7**, eabj8780.
9 X. Zhang, Y. Ran, Q. Fu and J. Ge, Ultrafast and Irreversibly Thermochromic SiO_2-PC/PEG Double Layer for Green Thermal Printing, *Small*, 2022, **18**, 2106533.
10 J. Zhou, P. Han, M. Liu, H. Zhou, Y. Zhang, J. Jiang, P. Liu, Y. Wei, Y. Song and X. Yao, Self-Healable Organogel Nanocomposite with Angle-Independent Structural Colors, *Angew. Chem., Int. Ed.*, 2017, **56**, 10462–10466.
11 Y. Zhang, L. Zhang, C. Zhang, J. Wang, J. Liu, C. Ye, Z. Dong, L. Wu and Y. Song, Continuous resin refilling and hydrogen bond synergistically assisted 3D structural color printing, *Nat. Commun.*, 2022, **13**, 7095.
12 Y. Sun, Y. Zhang, W. Yu, P. Jia, X. Zhang, N. Wu, H. Yu, Y. Song and J. Zhou, Bio-inspired stretchable and self-healable nanocomposite gelatin hydrogel with low silica nanoparticle content and brilliant angle/strain-independent structural colors, *Chem. Eng. J.*, 2024, **496**, 154190.
13 Y. Hu, C. Qi, D. Ma, D. Yang and S. Huang, Multicolor recordable and erasable photonic crystals based on on-off thermoswitchable mechanochromism toward inkless rewritable paper, *Nat. Commun.*, 2024, **15**, 5643.
14 J. Ge, G. James, H. Le, Z. Lu and Y. Yin, Rewritable Photonic Paper with Hygroscopic Salt Solution as Ink, *Adv. Mater.*, 2009, **21**, 4259–4264.
15 Q. Li, Z. Chen, Y. Zhang, S. Ding, H. Ding, L. Wang, Z. Xie, Y. Fu, M. Wei, S. Liu, J. Chen, X. Wang and Z. Gu, Imaging cellular forces with photonic crystals, *Nat. Commun.*, 2023, **14**, 7369.
16 Q. Lyu, M. Li, L. Zhang and J. Zhu, Structurally-colored adhesives for sensitive, high-resolution, and non-invasive adhesion self-monitoring, *Nat. Commun.*, 2024, **15**, 8419.
17 M. Qin, J. Li and Y. Song, Toward High Sensitivity: Perspective on Colorimetric Photonic Crystal Sensors, *Anal. Chem.*, 2022, **94**, 9497–9507.
18 K. Yuan, H. Li, R. Zuo, B. Gan and C. Xiong, Highly Sensitive Detection of Isomers through Dynamic Reflection Spectroscopy Based on Simple Amorphous Photonic Crystals, *J. Phys. Chem. C*, 2023, **127**, 19651–19658.
19 X. Pan, Z. Zhang, Y. Yun, X. Zhang, Y. Sun, Z. Zhang, H. Wang, X. Yang, Z. Tan, Y. Yang, H. Xie, B. Bogdanov, G. Zmaga, P. Senyushkin, X. Wei, Y. Song and M. Su, Machine Learning-Assisted High-Throughput Identification and Quantification of Protein Biomarkers with Printed Heterochains, *J. Am. Chem. Soc.*, 2024, **146**, 19239–19248.
20 J. Fonseca, L. Meng, P. Moronta, I. Imaz, C. López and D. Maspoch, Assembly of Covalent Organic Frameworks into Colloidal Photonic Crystals, *J. Am. Chem. Soc.*, 2023, **145**, 20163–20168.
21 J. M. Kim, Y. J. Jung, B. C. Park, B. Lim, H. Kong, J. M. Park, H. Lee and S. H. Jung, Photonic multilayers for ultrasensitive millisecond colorimetric discrimination between benzene, toluene, and xylene, *Sens. Actuators, B*, 2022, **351**, 130974.
22 D. Kou, W. Ma and S. Zhang, Functionalized Mesoporous Photonic Crystal Film for Ultrasensitive Visual Detection

and Effective Removal of Mercury(II) Ions in Water, *Adv. Funct. Mater.*, 2021, **31**, 2007032.

23 M. Lu, X. Zhang, D. Xu, N. Li and Y. Zhao, Encoded Structural Color Microneedle Patches for Multiple Screening of Wound Small Molecules, *Adv. Mater.*, 2023, **35**, 2211330.

24 C. Hu, J. Zhou, J. Zhang, Y. Zhao, C. Xie, W. Yin, J. Xie, H. Li, X. Xu, L. Zhao, M. Qin and J. Li, A structural color hydrogel for diagnosis of halitosis and screening of periodontitis, *Mater. Horiz.*, 2024, **11**, 519–530.

25 C. Zhang, J. Liu and C. Xiong, Detection of isomers based on silica colloidal crystals doped with noble metals, *J. Colloid Interface Sci.*, 2025, **691**, 137477.

26 C. Zou, Y. Xu, W. Long, Z. A. Zou and C. Xiong, Detection of topology freezing transition temperature of vitrimers based on photonic coatings from photonic crystals and vitrimers, *Opt. Mater.*, 2024, **157**, 116093.

27 W. Y. Wang, X. J. Zha, R. Y. Bao, K. Ke, Z. Y. Liu, M. B. Yang and W. Yang, Vitrimers of polyolefin elastomer with physically cross-linked network, *J. Polym. Res.*, 2021, **28**, 210.

28 Y. Yao, E. He, H. Xu, Y. Liu, Y. Wei and Y. Ji, Fabricating liquid crystal vitrimer actuators far below the normal processing temperature, *Mater. Horiz.*, 2023, **10**, 1795–1805.

29 W. Stöber, A. Fink and E. Bohn, Controlled growth of monodisperse silica spheres in the micron size range, *J. Colloid Interface Sci.*, 1968, **26**, 62–69.

30 Y. Wang, Q. He, Y. Hao, X. Ji, T. Wu, J. Li and C. Xiong, High-efficiency fabrication of uniform photonic crystals by a vertical deposition method from multiple glass slides of simple moulds and their application in isomer recognitions, *Opt. Mater.*, 2024, **152**, 115436.

31 Y. Yang, H. Wang, S. Zhang, Y. Wei, X. He, J. Wang, Y. Zhang and Y. Ji, Vitrimer-based soft actuators with multiple responsiveness and self-healing ability triggered by multiple stimuli, *Matter*, 2021, **4**, 3354–3365.

32 L. Peng, L. Hou and P. Wu, Synergetic Lithium and Hydrogen Bonds Endow Liquid-Free Photonic Ionic Elastomer with Mechanical Robustness and Electrical/Optical Dual-Output, *Adv. Mater.*, 2023, **35**, 2211342.